

# Nonlinear Modeling and Evaluation of Rolling Friction

Yoshihiro Maeda, Makoto Iwasaki, Motohiro Kawafuku, and Hiromu Hirai

Department of Computer Science and Engineering

Nagoya Institute of Technology

Gokiso, Showa, Nagoya 4668555, Japan

ymaeda@nitech.ac.jp

<http://mechatro.elcom.nitech.ac.jp/>

**Abstract**—This paper presents a nonlinear friction modeling and its evaluation for rolling friction behaviors in ball screw-driven table systems. The rolling friction behaves as a nonlinear component in the table drive mechanism, especially in the micro-displacement region, deteriorating the control performance in the fine positioning. The friction characteristic, therefore, should be clarified to provide the precise mathematical simulator and to design the effective compensators. In the friction modeling, the characteristics of rolling friction, which are depending on the displacement region, are especially paid attention: In “starting rolling displacement region”, the friction force dynamically varies for the displacement after velocity reversal. In “rolling region”, on the other hand, the friction force statically indicates the Coulomb friction. Based on the nonlinear behaviors, the rolling friction can be mathematically modeled, and the rolling friction model can express both the dynamic and static characteristics of friction after the reversal. The proposed nonlinear modeling of the rolling friction has been evaluated in both frequency and time domains using a prototype for industrial positioning devices.

## I. INTRODUCTION

The positioning requirements in a wide variety of high performance mechatronic systems, such as data storage devices, machine tools, and industrial robots, become more precisely. The mechanical vibration and nonlinear friction characteristics in positioning systems should be clarified to provide the precise mathematical simulator and to design the effective compensators.

The nonlinear friction in the mechanisms, i.e. rolling ball guide and bearing, which deteriorates the control performance, should be compensated to provide high-precision positioning. Nonlinear elastic characteristics of the rolling friction due to the deformations and slips in bearing balls, rolling ball guide, and/or lubricant grease are well-known to affect the positioning accuracy [1], [2], [3]. The rolling friction force depends on the rolling displacement after velocity reversal, and behaves as the transient characteristics in the following regions:

- Starting rolling displacement region

The friction force dynamically varies depending on displacement after the reversal, because rolling element, rolling ball guide, and/or lubricant grease deform and slip at the contact points between the rolling element and rolling ball guide.

- Rolling region

The rolling elements roll, and the friction force statically behaves as the Coulomb friction.

Varieties of researches on the rolling friction modeling and compensation have been done. For example, Otsuka proposed a measuring approach which could easily obtain the nonlinear elastic characteristic of rolling friction in bearings and rolling ball guides [4]. Koizumi also proposed a simple rolling friction model, which could simulate the rolling friction characteristics [5]. Swevers discussed, on the other hand, the nonlinear elastic behavior of rolling friction as an effect of pre-sliding, and proposed a friction model as a slip model [6], [7]. The authors have performed precise mathematical modelings, especially focusing on the nonlinear friction, for a prototype of ball screw-driven table positioning device which simulates actual mechatronic products, such as industrial robot handlers, semiconductor inspection equipments, etc. The modeling provided the precise simulator with the nonlinear elastic characteristic of rolling friction, and clarified the importance of compensation for the nonlinear friction in fast and precise positioning [8]. As the future work, the evaluation for the proposed rolling friction model in both frequency and time domains, is still remained to adopt the model to the controller design.

This paper presents a nonlinear friction modeling and its evaluation for the rolling friction behaviors in a laboratory prototype of ball screw-driven table positioning device. In the rolling friction modeling, the nonlinear elastic properties are especially paid attention, depending on the displacement regions in motion: In “starting rolling displacement region”, the friction force dynamically varies for the displacement after velocity reversal. In “rolling region”, on the other hand, the friction force statically behaves as the Coulomb friction. Based on the properties, the rolling friction model can be mathematically formulated, which can express both the dynamic and static characteristics in the friction. The proposed nonlinear model has been evaluated in both frequency and time domains using the prototype, where the bode characteristics of the plant system and the time responses in positioning were precisely reproduced by the simulator using the friction model. As the result of a series of the evaluations, the effectiveness of the proposed approach has been verified.

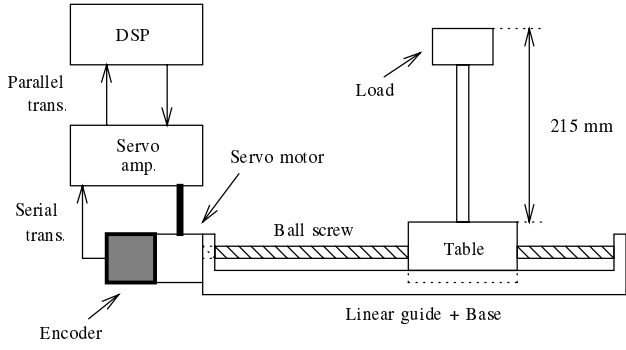


Fig. 1. System configuration of prototype.

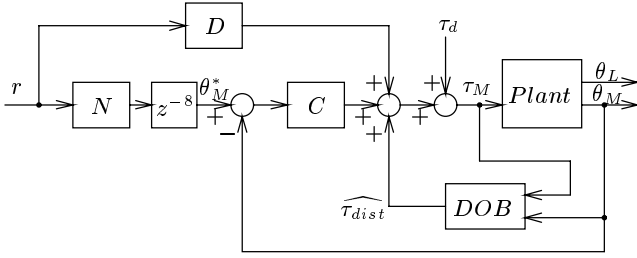


Fig. 2. 2DOF positioning system based on coprime factorization.

## II. POSITIONING SYSTEM AND FREQUENCY CHARACTERISTIC

### A. Configuration of table positioning system

Fig.1 shows the configuration of a target table positioning system as a prototype. The table with a flexible load is driven by an AC servo motor (rated output of 200 W and rated speed of 3,000 rpm) with a ball screw (length of 520 mm and pitch of 20 mm), where the table is guided by a rolling ball guide (a linear guide) on the base. Flexible mechanism in the load, consisting of a weight and a beam, excites resonant vibrations between the table, and simulates vibratory mechanisms in variety of industrial positioning devices. All the experimental evaluations using the prototype have been performed in a thermostatic room under the constant conditions in temperature of 25 °C and humidity of 40 %.

### B. Frequency characteristics of mechanism

Fig.2 shows a block diagram of 2 degrees-of-freedom positioning system based on coprime factorization with disturbance observer [9], where  $r$  is the position reference,  $\theta_M$  is the motor angular position,  $\theta_L$  is the load position,  $\tau_M$  is the motor torque reference as the control input,  $\tau_{dist}$  is the estimated disturbance,  $\theta_M^*$  is the motor angular position trajectory generated by a feedforward compensator, and  $\tau_d$  is the disturbance for the control input.  $N$  and  $D$  are the feedforward compensators which are mathematically designed by the coprime factorization of transfer characteristic of the motor position for the motor torque reference,  $z^{-8}$  is the dead time compensator based on the Smith method,  $C$  is the feedback PID compensator for a motor position error, and

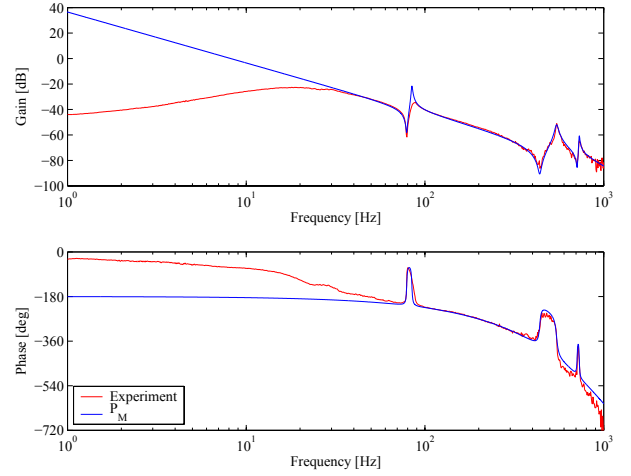


Fig. 3. Bode characteristics of motor position for torque reference.

$DOB$  is a disturbance observer. The reduction nominal plant model for the feedforward compensators and the disturbance observer is a 2-mass system which includes the vibration of 84 Hz as mentioned later [8]. The frequency bandwidth of the disturbance observer is determined by a 2nd-order low pass filter with bandwidth of 100 Hz. The gain cross frequency of open-loop frequency characteristic of the feedback system is about 100 Hz.

The bode analysis is performed by a FFT-analyzer using the motor torque reference (rated torque as of 3 V) as input and the motor position as output with the following condition: the position reference of  $r = 0$ , only PID controller in Fig.2, and sinusoidal signal to PID compensator output as the disturbance input :  $\tau_d$ .

Solid red lines in Fig.3 show a bode characteristic of the motor position for the motor torque reference with the sinusoidal signal amplitude of 1.2 V. There exist three remarkable vibration modes and a phase delay due to the servo amplifier in the high frequency range over 100 Hz. Solid blue lines indicate a mathematical linear plant model  $P_M(s)$  considering rigid mode, three vibration modes (84, 535, 722 Hz), and dead time components (dead time corresponds to 8 times of the control sample time :  $T_s = 166 \mu s$ ) [8]. The actual frequency characteristic shows the decrease in amplitude in the low frequency range under 30 Hz, due to effects of the nonlinear friction.

Fig.4 shows the bode characteristics of the plant for different trials in sinusoidal amplitude of the sinusoidal input signal. Black lines with the amplitude of 0.6 V indicate that smaller amplitude causes 1) higher in the corner angular frequency at some ten Hz and 2) smaller in the gain at 1st vibration mode, comparing to the red lines with 1.2 V amplitude. Green lines with 0.15 V amplitude, on the other hand, show the quite different characteristics from those of 0.6 V and 1.2 V, where the output motor position moves in the micro-displacement region, e.g. displacement amplitude less than 5  $\mu m$ . From the figure, the green lines indicate 1) constant amplitude until the

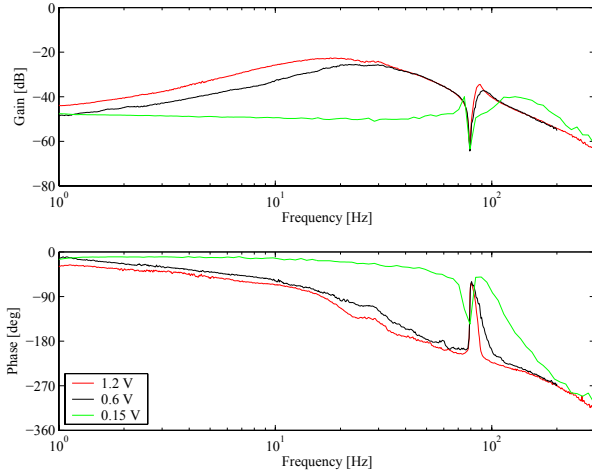


Fig. 4. Bode characteristics for different input amplitude.

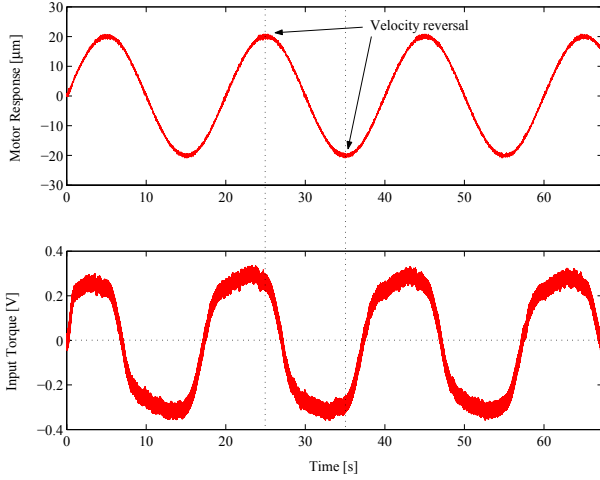


Fig. 5. Response waveforms of motor position and torque reference for sinusoidal position command.

1st vibration mode frequency and 2) 2nd-order delay behavior with a resonant frequency at 120 Hz [1], [10]. This different characteristic in the micro-displacement region is caused by the rolling friction properties due to the nonlinear behaviors with total moment inertia in motor and load, and nonlinear elastic components in the mechanism. In the following chapter, the nonlinear elastic behaviors are precisely analyzed, and formulated as a rolling friction model.

### III. PRECISE NONLINEAR MODELING BY ROLLING FRICTION

#### A. Nonlinear elastic characteristic of rolling friction

The rolling friction behaves as the nonlinear elastic component in the micro-displacement region, due to the deformations and slips in the contact points of bearing balls and rolling ball guide in the micro-displacement region [4]. In order to clarify the rolling friction characteristic, the response waveforms of the motor torque reference and the motor position in the

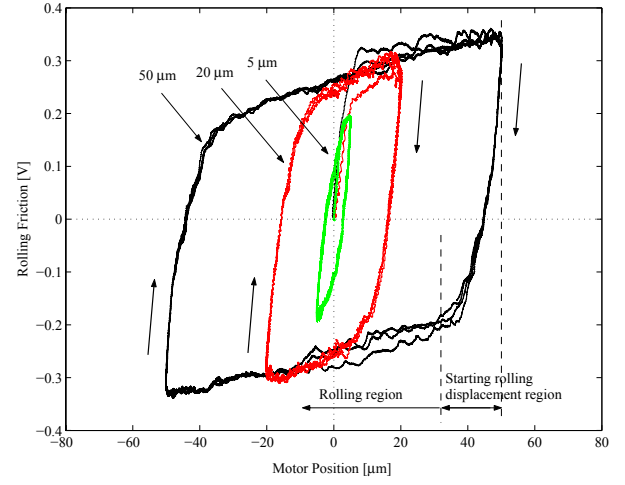


Fig. 6. Nonlinear elastic behaviors of rolling friction for motor position.

positioning are measured, where the PID feedback controller as same as in II-B are used with the sinusoidal position reference whose frequency is as of 0.05 Hz. Fig.5 shows an example of response waveforms for the sinusoidal reference amplitude of 20  $\mu\text{m}$ . From the figure, it is obvious that the friction behaves as nonlinear properties, i.e. the positive or negative force of about  $\pm 0.25$  V can keep until the velocity reversal. Fig.6, on the other hand, Lissajous's figures for Fig.5 are given to clarify the nonlinear behaviors, where different cases with sinusoidal amplitude of 5 and 50  $\mu\text{m}$  are indicated together. The figures clearly indicate that the friction can be characterized by the nonlinear elastic component with hysteresis property. The friction behaves in two regions: in "starting rolling displacement region", the bearing ball can not perfectly roll and the rolling friction behaves as a nonlinear elastic characteristic. In "rolling region", on the other hand, the bearing ball rolls, resulting in a hysteresis characteristic at velocity reversal points. It is well-known that the shape of hysteresis is constant independent of the displacement and the initial position in motion [11].

#### B. Rolling friction model

The rolling friction characteristic can be mathematically modeled as follows, considering the Coulomb friction:

- Rolling friction

$$F_{\text{rolling}}(\delta) = \begin{cases} \text{sgn}(\omega_M)(2T_{fc}g(\xi) - F_{r0}) & : |\delta| < \theta_r \text{ and } |F_{\text{rolling}}| < T_{fc} \\ \text{sgn}(\omega_M)T_{fc} & : |\delta| \geq \theta_r \text{ or } |F_{\text{rolling}}| \geq T_{fc} \end{cases}, \quad (1)$$

$$g(\xi) = \begin{cases} \frac{1}{2-n}(\xi^{n-1} - (n-1)\xi) & : n \neq 2 \\ \xi(1 - \ln \xi) & : n = 2 \end{cases}, \quad (2)$$

$$\delta = |\theta_M - \delta_0|, \quad \xi = \delta/\theta_r, \quad (3)$$

where  $F_{\text{rolling}}(\delta)$  is the rolling friction force,  $T_{fc}$  is the Coulomb friction force,  $\theta_r$  is the width of starting rolling displacement region,  $n$  is a coefficient which determines the

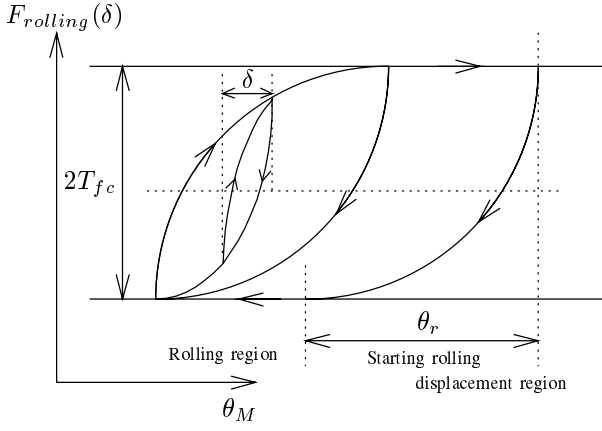


Fig. 7. Rolling friction characteristic.

swelling of hysteresis,  $\text{sgn}(\cdot)$  is the sign function,  $\delta$  is the displacement after reversal, and  $F_{r0}$  and  $\delta_0$  are the rolling friction force and the motor displacement at reversal, respectively.

Fig.7 shows a conceptual characteristic of the rolling friction model. This rolling friction model can express both the dynamic and static characteristics in friction after reversal: the hysteresis characteristic expresses the dynamic rolling friction during  $|\delta| < \theta_r$ , and the Coulomb friction  $T_{fc}$  behaves as the static friction in the range of  $|\delta| \geq \theta_r$ .

#### C. Parameterization of rolling friction model

The parameters, to be identified in the rolling friction model, are three:  $T_{fc}$ ,  $\theta_r$  and  $n$ . Here, the parameters are determined by the following steps, in order to precisely simulate the actual characteristics:

1.  $T_{fc}$  can be determined as the Coulomb friction force by conventional measurement approach with a constant velocity drive.
2.  $\theta_r$  can be determined by the width of starting rolling displacement region, which is directly measured by the waveforms in Fig.6 at velocity reversal.
3.  $n$  can be tuned by trial and error, to simulate the actual hysteresis form [11].

In the prototype system, the parameters are set as  $T_{fc} = 0.25$  V,  $\theta_r = 30 \mu\text{m}$ , and  $n = 1.62$ .

### IV. EVALUATION OF THE ROLLING FRICTION MODEL

#### A. Definition of friction models

In order to evaluate the proposed rolling friction model, two plant mathematical models, “Model-1” and “Model-2”, are defined and compared. Model-1 is composed of the linear plant as shown by the blue lines in Fig.3 and the following conventional static nonlinear friction including the Stiction force, the Stribeck effect, the Coulomb friction, and the viscous friction:

- Stiction force and Stribeck effect

$$F_{static} = \begin{cases} u & \text{if } |u| \leq T_{fs} \text{ at } \omega_M = 0 \\ (T_{fs} - T_{fc})e^{-\omega_M^2/\omega_s} & \omega_M \neq 0 \end{cases}, \quad (4)$$

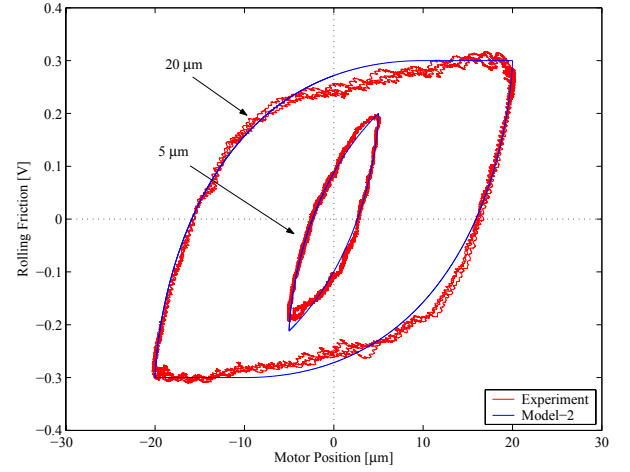


Fig. 8. Nonlinear elastic behaviors of rolling friction.

- Coulomb friction

$$F_{coulomb} = \begin{cases} \text{sgn}(\omega_M) T_{fc} & : |\omega_M| \geq \Delta\omega \\ \text{sgn}(\omega_M) T_{fc} \omega_M / \Delta\omega & : |\omega_M| < \Delta\omega \end{cases}, \quad (5)$$

- viscous friction

$$F_{viscous} = D_v \omega_M, \quad (6)$$

where  $u$  is the motor torque reference,  $\omega_M$  is the motor angular velocity,  $T_{fs}$  is the Stiction force,  $D_v$  is the viscous friction coefficient,  $\omega_s$  is the Stribeck angular velocity, and  $\Delta\omega$  is the micro-velocity. The parameters of the static friction model in eqs.(4)-(6) for the prototype have been identified experimentally as  $T_{fs} = 0.58$  V,  $D_v = 2.1 \times 10^{-2}$  Vs/rad,  $\omega_s = 4.7$  rad/s, and  $\Delta\omega = 0.1$  rad/s.

Model-2, on the other hand, the rolling friction model in eqs.(1)-(3) is added to Model-1.

#### B. Evaluation in micro-displacement region

Fig.8 shows a comparative evaluation for the nonlinear elastic characteristic between actual and model responses as Lissajous's figures, where the motion conditions are the same as of in II-B with the sinusoidal frequency of 0.05 Hz. From the figure, blue lines by Model-2 can well-simulate the actual characteristics indicated by red lines in both cases of the sinusoidal amplitude of 5 and 20  $\mu\text{m}$ , concerning the hysteresis slopes in the starting rolling displacement region.

#### C. Evaluation in frequency domain

Here, the bode characteristics of the plant are evaluated for different input sinusoidal amplitude, especially paying attention to the corner angular frequency, the resonant mode gain, and the 2nd-order delay behavior in micro-displacement region, as stated in II-B. Fig.9 shows the bode characteristics of the plant with input sinusoidal amplitude of 1.2 V. From the figure, blue lines by Model-2 can precisely express the actual characteristic indicated by red lines, for both the corner

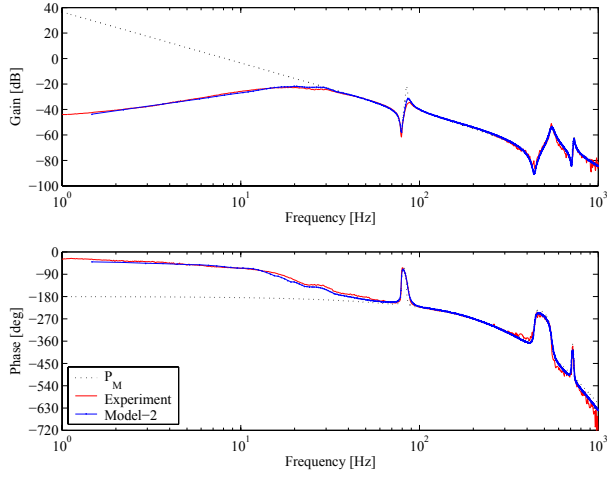


Fig. 9. Bode characteristics of motor position for torque reference with amplitude of 1.2 V.

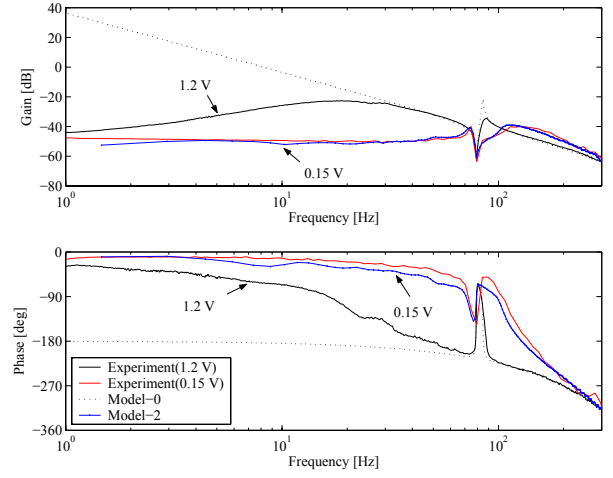


Fig. 11. Bode characteristics of motor position for torque reference with amplitude of 0.15 V.

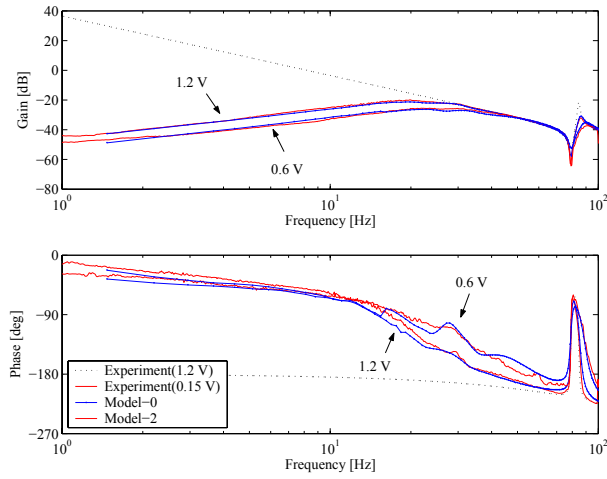


Fig. 10. Bode characteristics of motor position for torque reference with amplitude of 0.6 V and 1.2 V.

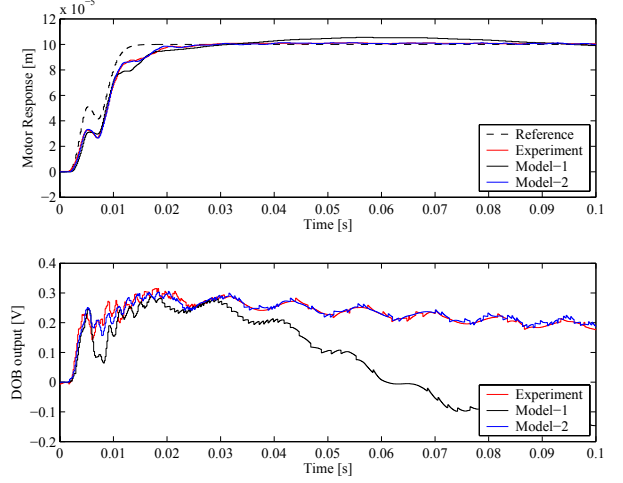


Fig. 12. Response waveforms of motor position and estimated friction.

angular frequency at about 30 Hz and the decrease in gain at the 1st vibration mode. Fig.10 shows the comparative bode characteristics for different amplitude in the sinusoidal input. In the figure, 0.6 and 1.2 V in amplitude have been given as the same manner as of in Fig.4, where the characteristics have been magnified below the 1st vibration mode. Model-2 indicated by blue lines can reproduce the decrease in the corner angular frequency corresponding to the decrease in the input amplitude.

In Fig.11, on the other hand, the bode characteristic in the motion range of the micro-displacement region has been evaluated by giving the sinusoidal input amplitude of 0.15 V. From the figure, the quite different characteristic from the one with 1.2 V, which behaves as the 2nd-order delay property, can be precisely reproduced by Model-2 with the alternative resonant frequency at 120 Hz. As the result of series of evaluations in Figs.9-11, the proposed rolling friction model

can simulate the actual frequency characteristics, resulting in a precise simulator in the frequency domain.

#### D. Evaluation in the positioning response

In order to verify the dynamic friction behavior at the starting rolling movement and velocity reversal, the positioning time response has been numerically simulated using the proposed friction model. Fig.12 shows the response waveforms of the motor position and the estimated friction by the disturbance observer during positioning, where the position reference with amplitude of 0.1 mm in table position has been given to the 2DOF controller shown in Fig.2. In the figure, black broken line indicates the motor position trajectory reference  $\theta_M^*$  generated by the feedforward compensator, red lines show the actual responses, and blue lines show the simulated responses by Model-2. Here, in order to clarify the effectiveness of the proposed rolling friction model, the simulated responses using Model-1 are comparatively indicated by black solid lines.

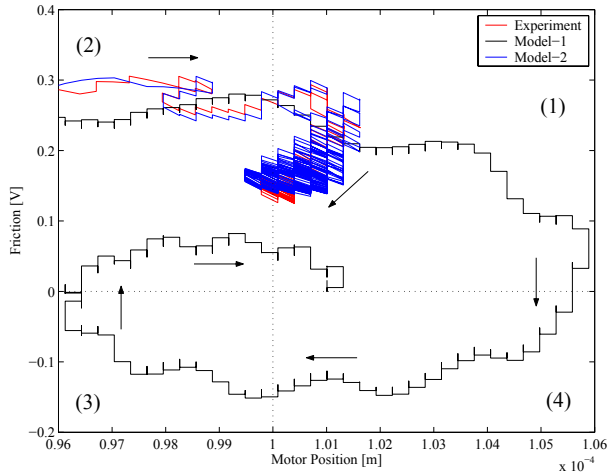


Fig. 13. Friction characteristics for displacement around target position.

From the figure, the responses in the Model-1 can follow the actual responses during the acceleration and deceleration until the settling. In the settling region ( $t > 20$  ms), however, the friction response by Model-1 become quite different from the experimental one. The responses by Model-2, on the other hand, can precisely follow the actual ones from the starting until the settling.

In order to examine the difference in friction responses at the settling, a friction characteristic for the motor position has been depicted as a Lissajous's figure in Fig.13, by using the same data as of Fig.12. In the figure, a vertical dotted line indicates the target position of 0.1 mm, the regions (1) and (4) denote an overshoot response in motor position, and the regions (3) and (4) correspond to the negative friction force. Red line of actual response in Fig.13 gets back only in region (1) in spite of the overshoot, maintaining the positive friction force without the direction reversal in friction force, and the nonlinear elastic characteristic clearly exists. Black line, indicating the simulator response with Model-1, generates the negative friction in regions (3) and (4) at the direction reversal due to the overshoot in response, and can not express the actual friction response. The proposed model of Model-2 considering the rolling friction, on the other hand, can reproduce the actual motion with the accuracy within  $1 \mu\text{m}$  in motor position, operating only in region (2) for the velocity reversal.

## V. CONCLUSIONS

In this paper, a nonlinear friction modeling and its evaluation for rolling friction behaviors were presented for the prototype of ball screw-driven table system. The rolling friction with the nonlinear elastic properties was mathematically modeled as the dynamic friction, and the proposed model was evaluated in both frequency and time domains as the bode characteristics and the time responses in positioning. As the result of a series of evaluations, the effectiveness of the proposed approach was verified.

## REFERENCES

- [1] J.Otsuka: "Present and Future Technique of Ultraprecision Positioning", *JSPE*, Vol.61, No.12, pp.1645-1649 (1995)
- [2] S.Futami, A.Furutani: "Nanometer Positioning Using AC Linear Motor and Rolling Guide (1st Report) -System Set-up and Coarse/Fine Positioning-", *JSPE*, Vol.57, No.3, pp.158-163 (1991)
- [3] J.Swevers, F.Al-Bender, C.G.Gansemann, T.Prajogo: "An Integrated Friction Model Structure with Improved Presliding Behavior for Accurate Friction Compensation", *IEEE Trans. on Automatic Control*, Vol.45, No.4, pp.675-686 (2000)
- [4] J.Otsuka, I.Aoki, T.Ishikawa: "A Study on Nonlinear Spring Behavior of Rolling Elements (1st Report) -Two Simple Measuring Methods-", *JSPE*, Vol.66, No.6, pp.944-949 (2000)
- [5] T.Koizumi, O.Kuroda: "Analysis of Damped Vibration of a System with Rolling Friction -Rolling Friction Depends on the Displacement-", *Journal of Japanese Society of Tribologists*, Vol.35, No.6, pp.435-439 (1990)
- [6] F.Al-Bender, V.Lampaert, J.Swevers: "The Generalized Maxwell-Slip Model: A Novel Model for Friction Simulation and Compensation", *IEEE Trans. on Automatic Control*, Vol.50, No.11, pp.1883-1887 (2005)
- [7] Z.Jamaludin, H.Van Brussel, J.Swevers: "Quadrant Glitch Compensation using Friction Model-Based Feedforward and an Inverse-Model-Based Disturbance Observer", *IEEE Proc. of the 10th International Workshop on Advanced Motion Control*, Italy, pp.212-217 (2008)
- [8] M.Iwasaki, Y.Maeda, M.Kawafuku, H.Hirai: "Improvement of Precise Positioning Performance by Modeling and Compensation for Nonlinear Friction", *T. IEE Japan*, Vol.126-D, No.6, pp.732-740 (2006)
- [9] T.Umeno and Y.Hori: "Robust Speed Control of DC Servomotors Using Modern Two Degrees-of-Freedom Controller Design", *IEEE Trans. on IE*, Vol.38, No.5, pp.363-368, (1991)
- [10] S.Futami, A.Furutani: "Nanometer Positioning Using AC Linear Motor and Rolling Guide (2nd Report) -Tribology of the Rolling Guide-", *JSPE*, Vol.57, No.10, pp.106-111
- [11] S.Nakagawa, Y.Hamada: "Using a Friction Observer to Compensate Friction Force at Head Actuator Bearings of Magnetic Disk Drives", *JSME(C)*, Vol.66, No.642, pp.213-218 (2000)